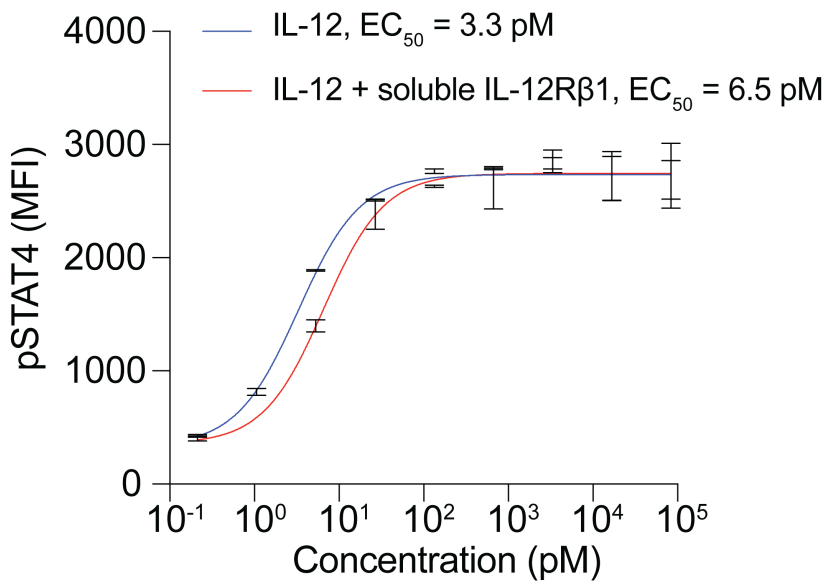
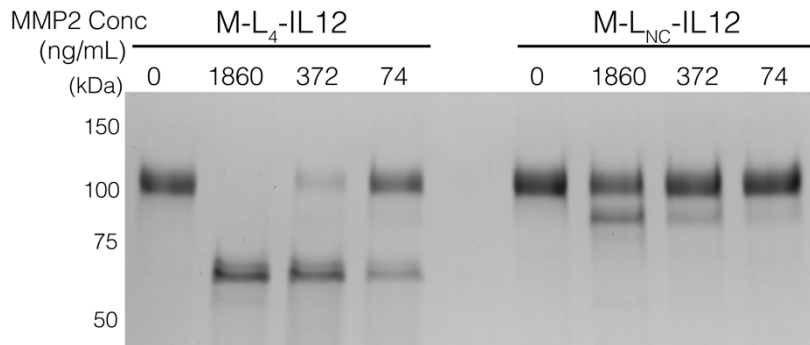
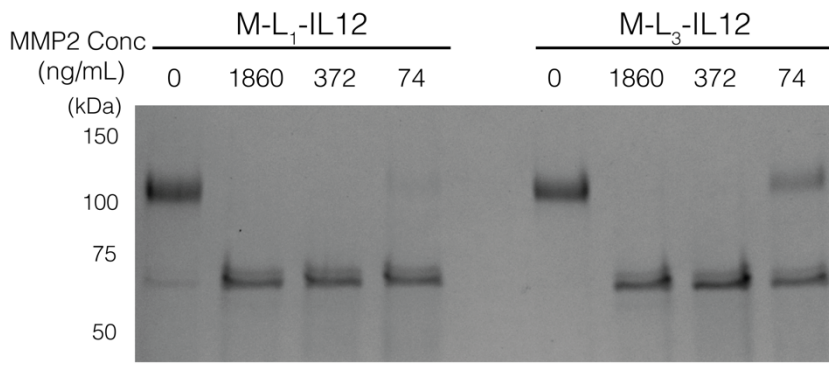


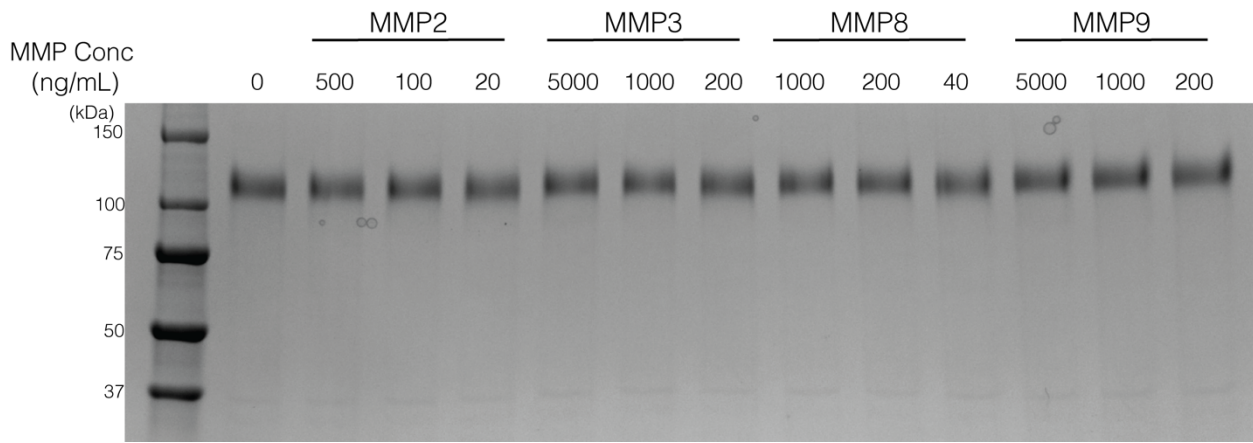
**Supplementary Fig. 1 | Size-exclusion chromatograms of affinity-purified masked IL-12 constructs. a,** Molecular schematic of masked IL-12. (His)<sub>6</sub>-tagged masked IL-12 constructs containing (G<sub>3</sub>S)<sub>2</sub> (**b**), (G<sub>3</sub>S)<sub>5</sub> (**c**), and (G<sub>3</sub>S)<sub>11</sub> (**d**) linkers between the mask and the p35 were expressed in HEK-293F cells and purified via Nickel-based affinity purification as described in the Materials and Methods. After elution, samples were loaded on size-exclusion columns to determine the optimal length between the mask and the p35 subunit. The masked IL-12 molecule in (**b**) was mostly eluted in aggregates and dimers. The masked IL-12 molecule in (**c**) still contained some dimer population at ~65 mL whereas the masked IL-12 containing (G<sub>3</sub>S)<sub>11</sub> linker (**d**) was homogenous monomer.



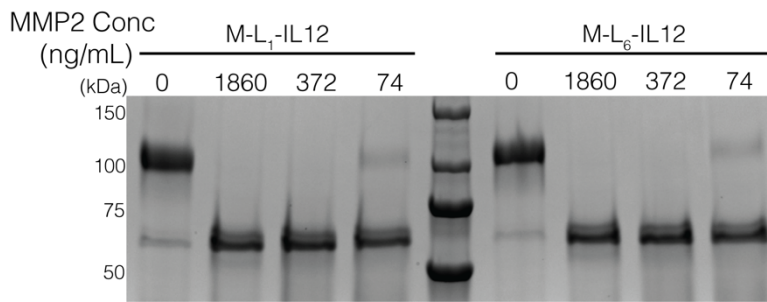
**Supplementary Fig. 2 | Soluble IL-12R $\beta$ 1 does not abrogate the IL-12 signaling when kept at equimolar ratios.** IL-12 and extracellular portion of IL-12R $\beta$ 1 were incubated for 1 hr at 37 C $^\circ$  to allow for complex formation. Pre-activated primary mouse CD8 $^+$  T cells were then treated for 15 min with either IL-12 alone or the preincubated complex of IL-12 and the IL-12R $\beta$ 1 (1:1 molar ratio, where the mixture of IL-12 + IL-12R $\beta$ 1 was serially diluted). Cells were fixed and stained for pSTAT4 as described in the Materials and Methods. Data are mean  $\pm$  s.e.m; n = 2 per condition (technical duplicates); each dilution of cytokine or cytokine-receptor complex was assessed in duplicate.  $EC_{50}$ , half-maximum effective concentration. The experiment was performed twice, with similar results.



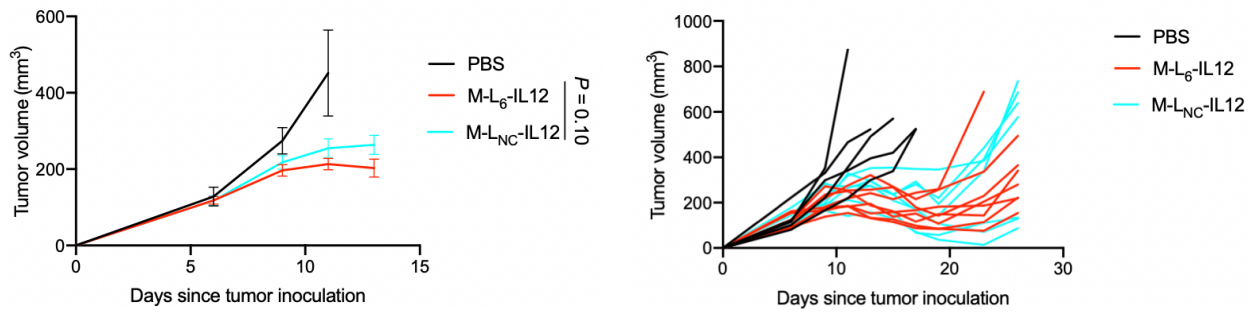
**Supplementary Fig. 3 | Protease substrates affect the efficiency of linker cleavage by MMP2.** Masked IL-12 constructs were diluted to a final concentration of 75 mg/mL (or 0.83 mM) and incubated with the indicated concentration of activated MMP2 for 30 min at 37°C. Samples were then immediately denatured by boiling with non-reducing SDS-PAGE buffer and loaded for electrophoresis. MMP2 at 74 ng/mL (~1 nM) is able to fully cleave M-L<sub>1</sub>-IL12, whereas some intact M-L<sub>3</sub>-IL12 is present. M-L<sub>4</sub>-IL12 contains only one MMP-responsive substrate, and thus, is only partially processed at that MMP2 concentration. Some degradation of the non-cleavable M-L<sub>NC</sub>-IL12 is observed, which may be due to nonspecific cleavage of IL-12Rb1. The experiment was performed twice with similar results.



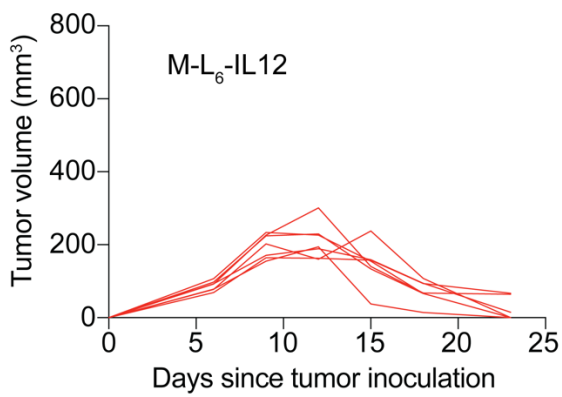
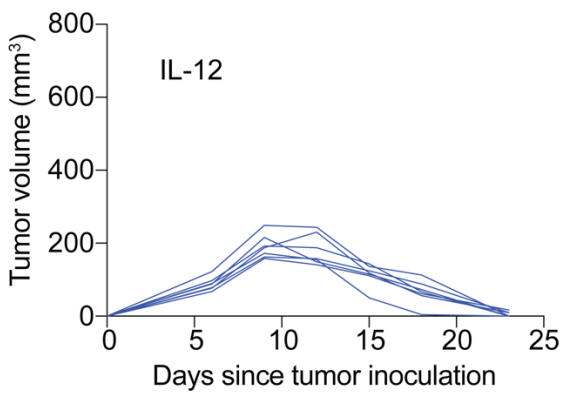
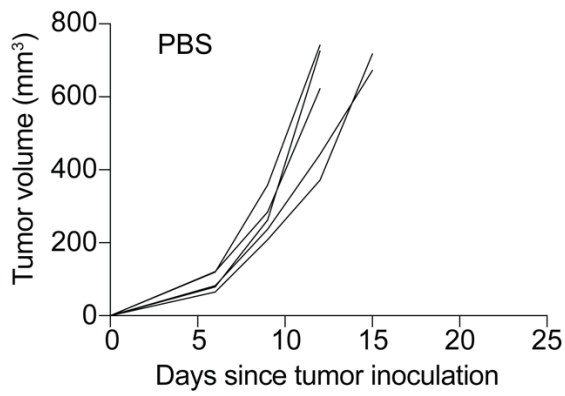
**Supplementary Fig. 4 | MMPs do not cleave SP-sensitive M-L<sub>2</sub>-IL12.** M-L<sub>2</sub>-IL12, which contains three repeats of LSGRSDNH, was diluted to 45 mg/mL (or 0.5 mM) and incubated with the indicated MMPs for 1 hr at 37 °C. Samples were then loaded on the gel and analyzed. Experiment was performed twice with similar results.



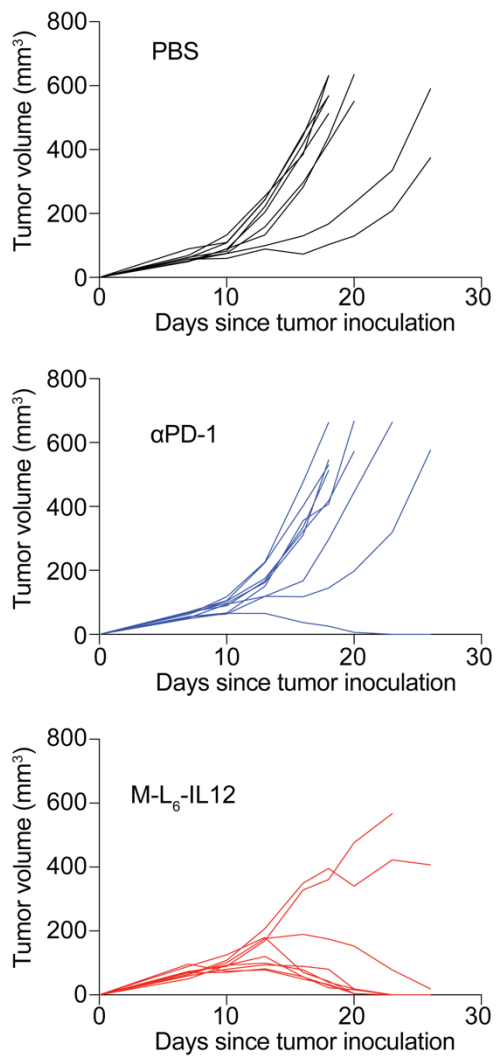
**Supplementary Fig. 5 | M-L<sub>1</sub>-IL12 and M-L<sub>6</sub>-IL12 are equally cleaved by MMP2.** Indicated amounts of activated MMP2 was incubated with 150 mg/mL (1.67 mM) of masked IL-12 construct for 30 min at 37 °C. Molecules were then loaded on the gel and analyzed. Experiment was performed twice with similar results.



**Supplementary Fig. 6 | Comparison of antitumor efficacy of non-cleavable (L<sub>NC</sub>) linker versus cleavable L<sub>6</sub> linker in MC38 model.** 7 days after inoculation of MC38 cells, mice were treated once with either PBS (n=5), 83.3 pmol M-L<sub>6</sub>-IL12 (n=7) or 83.3 pmol M-L<sub>NC</sub>-IL12 (n=7) i.v. Average tumor volumes (left) and individual growth curves (right) are shown. Considerable antitumor activity of M-L<sub>NC</sub>-IL12 may be attributed to the attenuation of IL-12 signaling, where (G<sub>3</sub>S)<sub>11</sub> linker's flexibility allows M-L<sub>NC</sub>-IL12 to activate CD8<sup>+</sup> T cells expressing high affinity IL-12 receptor (thereby promoting antitumor immunity)<sup>18</sup>.

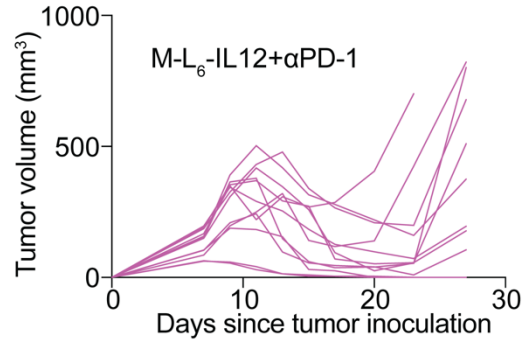
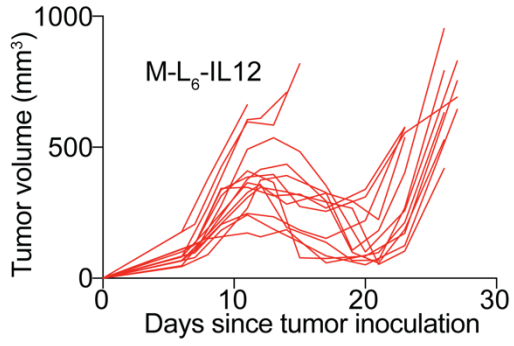
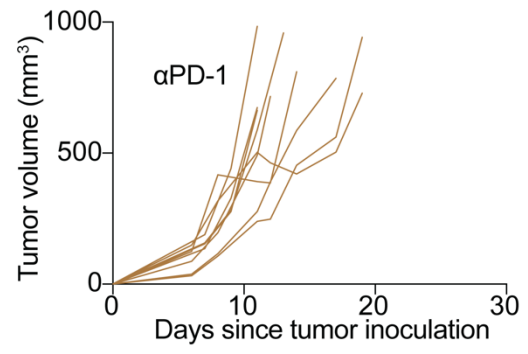
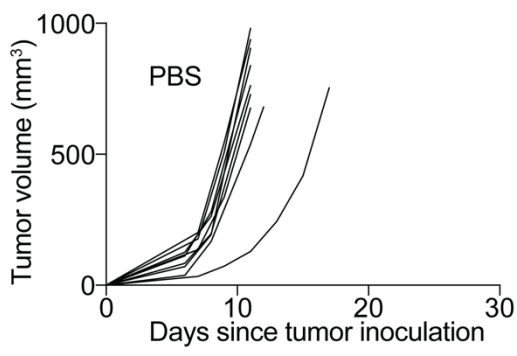


**Supplementary Fig. 7 | Unmodified IL-12 and M-L<sub>6</sub>-IL12 are equally efficacious in MC38 colon cancer model.** Mice were treated as described in Fig. 2b. Individual tumor curves are shown.

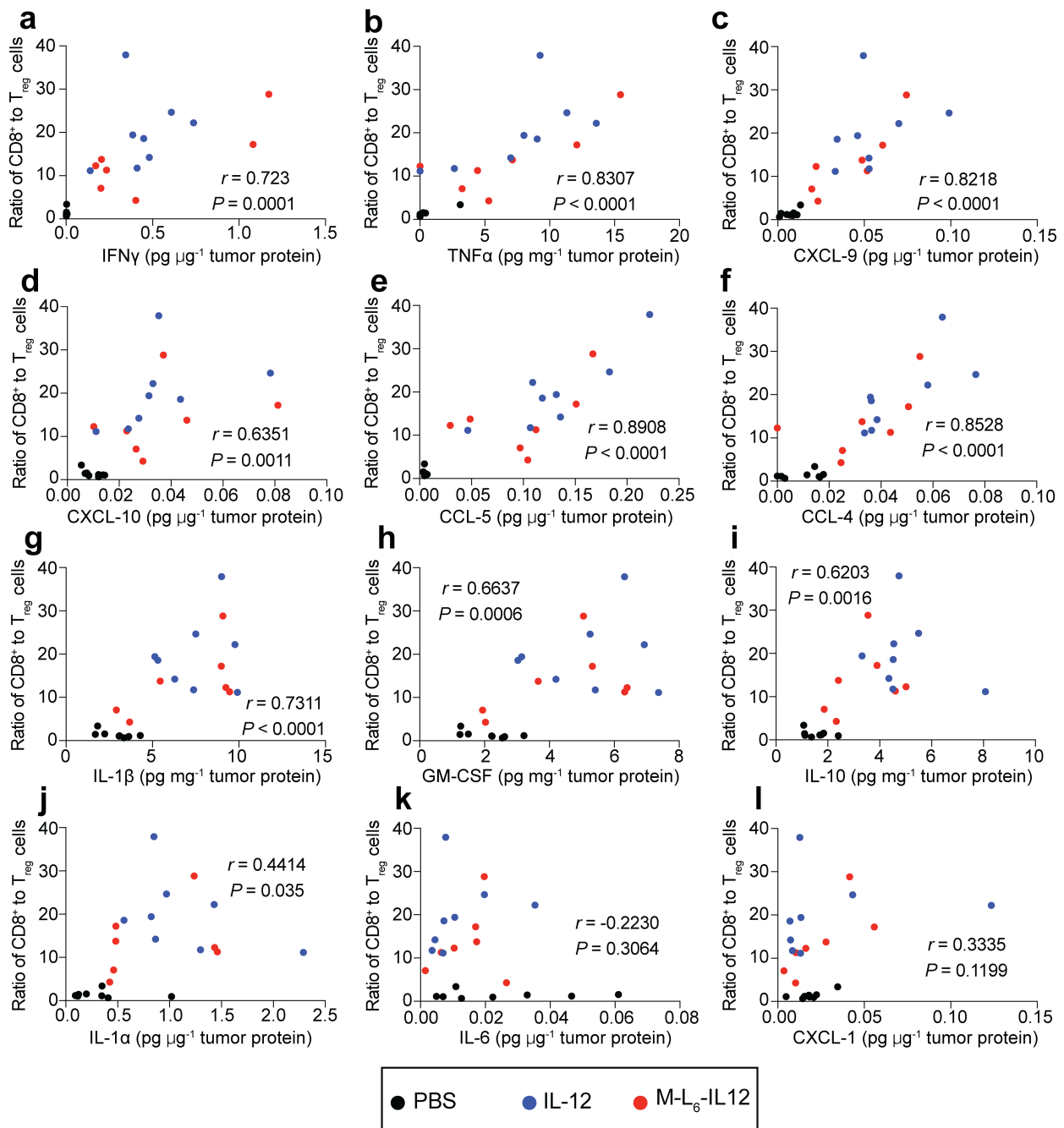


**Supplementary Fig. 8 | M-L<sub>6</sub>-IL12 is more efficacious than αPD-1 antibody in the CPI-resistant, EMT6 orthotopic tumor model.** Mice were treated as described in Fig. 2c. Individual tumor curves are shown.

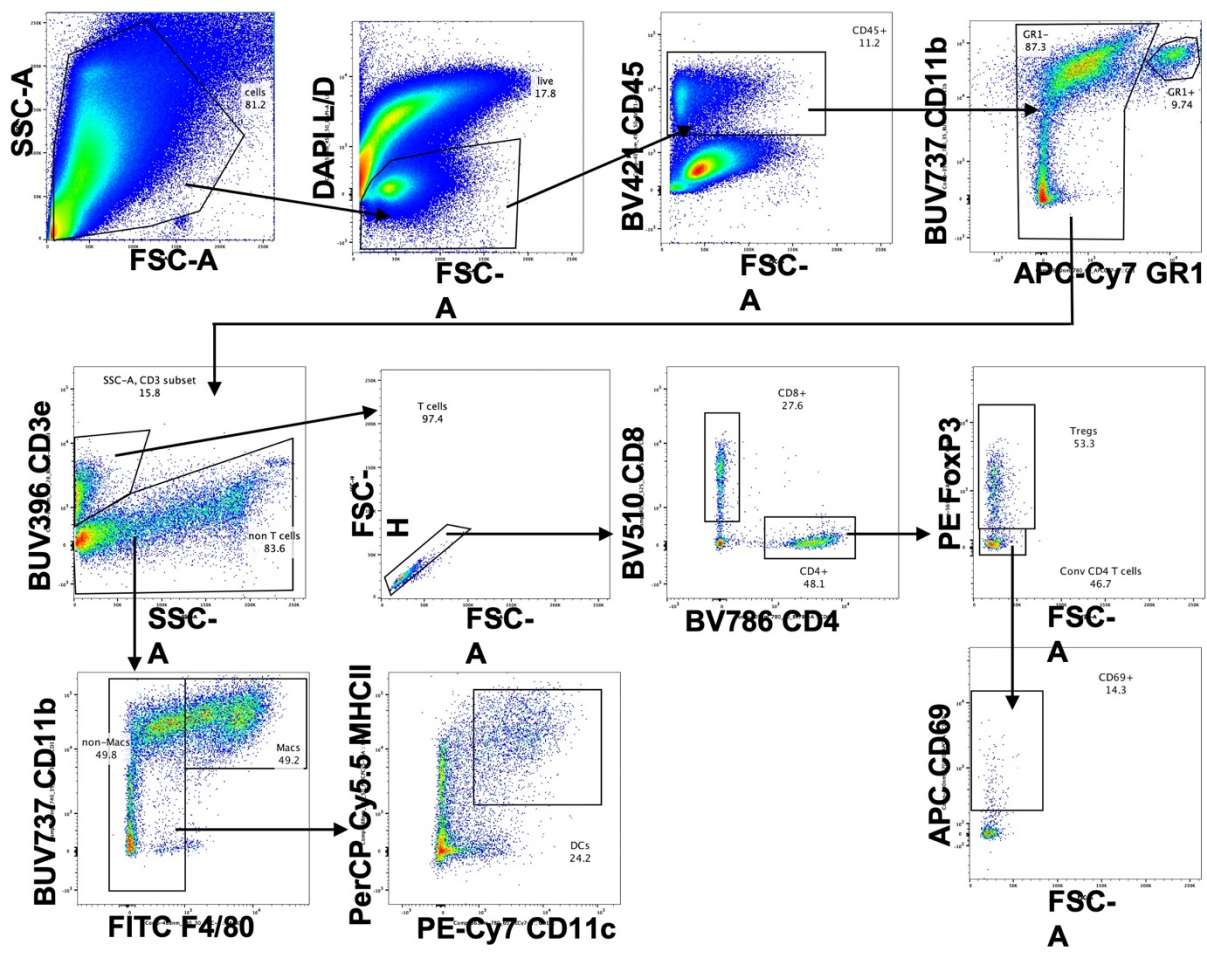




**Supplementary Fig. 9 | Combination of M-L<sub>6</sub>-IL12 and αPD-1 produces a stronger antitumor response than either agent alone.** Mice were treated as described in Fig. 2d. Individual tumor curves are shown.



**Supplementary Fig. 10 | Correlation analysis between various cytokines/chemokines and CD8<sup>+</sup> to T<sub>reg</sub> ratio.** a–l, Pearson correlation was performed using data presented in Fig. 3. Two-tailed  $P$  value and  $r$  value were obtained using Pearson correlation analysis on Prism Graphpad.



Supplementary Fig. 11 | Representative gating strategy for identifying immune cells present in B16F10 melanoma tumors. Macs = macrophages; DCs = dendritic cells.